Spectral Characteristics of CN Radical (B → X) and Its Application in Determination of Rotational and Vibrational Temperatures of Plasma

2011 Chinese Phys. Lett. 28 044703

(http://iopscience.iop.org/0256-307X/28/4/044703)

CHIN. PHYS. LETT. Vol. 28, No. 4 (2011) 044703

Spectral Characteristics of CN Radical ($B \to X$) and Its Application in Determination of Rotational and Vibrational Temperatures of Plasma

PENG Zhi-Min(彭志敏)[1], DING Yan-Jun(丁艳军)[1**], ZHAI Xiao-Dong(翟晓东)[1], YANG Qian-Suo(杨乾锁)[2], JIANG Zong-Lin(姜宗林)[2]

[1]*State Key Laboratory of Power Systems, Department of Thermal Engineering, Tsinghua University, Beijing 100084*
[2]*Laboratory of High Temperature Gas Dynamics, Institute of Mechanics, Chinese Academy of Sciences, Beijing 100190*

(Received 18 July 2010)

The aim is to resolve the difficulties of measurement of temperature at several thousands of Celsius degrees for some unstable non-equilibrium gas flows. Based on the molecular spectroscopy theory and inherent molecular structure characteristics of the CN radical, the dependence of the spectral profile on the rotational temperature (RT), vibrational temperature (VT) and optical apparatus function are numerically explored within some certain ranges. Meanwhile, by comparing the numerically calculated spectra with the experimental spectra of the CN radical, the corresponding RT and VT of the plasma induced by the interaction of the laser pulse from an oscillated Nd:YAG laser with the coal target are determined, respectively. In addition, a short discussion on the thermodynamic state and the energy transfer process of the CN radical is also given.

PACS: 47.80.Fg, 42.65.Re, 33.70.−w DOI: 10.1088/0256-307X/28/4/044703

High temperature phenomena have been studied widely and deeply with the progress of science and technology.[1−4] As the temperature rises to several thousands of Celsius degree for some unstable non-equilibrium gas flows, the characteristics on the heat kinetics and molecular dynamics are much more complex than those at room temperature. The excitation of molecules occurs in all freedoms such as the rotation level, vibration level and electronic level of these gaseous molecules. Therefore, the traditional thermodynamics is no longer suitable for the description and expression of the characteristics of these hot molecules. Meanwhile, the concept of translational temperature and the methods of temperature measurement are also limited so that they are of no concern for the gases with a high temperature.

Fortunately, the CN radical can broadly be found in a high temperature environment, such as in the universe,[5−10] re-entry environment,[11−14] supersonic combustion, plasma, gas phase reactions and so on.[15−19] Meanwhile, the limited lifetime of the CN radical at the upper levels results in the radiation transition from the upper level to the low level and the corresponding emission spectra contain the temperature and concentration information of the CN radical. Therefore, some primary parameters such as temperature and concentration can be estimated by analyzing the emission spectra such as the $B^2\sum^+ \to X^2\sum^+$ band of the CN radical. This physical mechanism is also the basis for the measurement of the rotational temperature (RT) and vibrational temperature (VT) for plasma under a high temperature.

In this Letter, based on the inherent molecular structure characteristics of the CN radical, dependences of intensity distribution of the $B^2\sum^+ \to X^2\sum^+$ band on the RT, VT and optical apparatus function (OAF) are numerically explored. At the same time, compared the experimental spectra with the numerical spectra and considered the OAF of the optical multi-channel analyzer used in the experiment, the RT and VT of a plasma induced by the interaction of the laser pulse from a free oscillated Nd:YAG laser with the coal target are determined.

According to the selection rules of the $B^2\sum^+ \to X^2\sum^+$ transitions, the intensity of a spectral line for the transition between two levels $(v', J' \to v'', J'')$ is expressed as[20−24]

$$I_{v''J''}^{v'J'} = N_{v'J'} A_{v''J''}^{v'J'} hc v_{v''J''}^{v'J'}, \tag{1}$$

where (v', J') and (v'', J'') represent the vibrational and rotational quantum numbers in the upper level and lower level, respectively, h is Planck's constant, c is the speed of light in vacuum, $v_{v''J''}^{v'J'}$ is the transition frequency (cm^{-1}); $N_{v'J'}$ is the molecule number in the upper level and obeys the Boltzmann distribution; $A_{v''J''}^{v'J'}$ is the Einstein emission coefficient (s^{-1}) expressed as

$$A_{v''J''}^{v'J'} = \frac{64\pi^4}{3h} \frac{S_{J''}^{J'}}{2J'+1} p_{v''J''}^{v'J'} \left(v_{v''J''}^{v'J'}\right)^3, \tag{2}$$

with $p_{v''J''}^{v'J'} = \left[\int_{-\infty}^{+\infty} \Psi_{v'J'}(r) R_e(r) \Psi_{v''J''}(r) dr\right]^2$, $\Psi_{vJ}(r)$ the ro-vibrational wave functions and $R_e(r)$ the electronic transition moment, $S_{J''}^{J'}$ the Honl–London factor.

Figure 1 shows the distributions of the spectral line intensity for different vibrational transitions with $T_e = T_v = T_r = 3000\,\mathrm{K}$. The largest intensity is defined as the value of 1000. From the data in Fig. 1, it is obvious that intensity of the 0-0 transition is stronger than that of the others and the distributions of the spectral line of all vibrational transitions are similar.

For a spectroscopy, the experimental spectra are not only affected by RT and VT but also by OAF. To determine the RT and VT, calibration of OAF is performed first. A mercury lamp or a laser with a

**Email: dyj@tsinghua.edu.cn

wavelength of 532 nm is utilized for the measurement of OAF before the spectrum experiment is performed. In many cases, OAF can be well fitted to a Gaussian profile as a function of the wavelength λ; therefore the best way to mathematically represent OAF is to consider a Gaussian profile given by[25]

$$G(\lambda) = \exp\left(- 4\ln 2 \cdot \frac{(\lambda - \lambda_0)^2}{(\Delta/2)^2} \right) \qquad (3)$$

where λ_0 is the central wavelength, Δ is the half-width and is about 0.321 nm in this study.

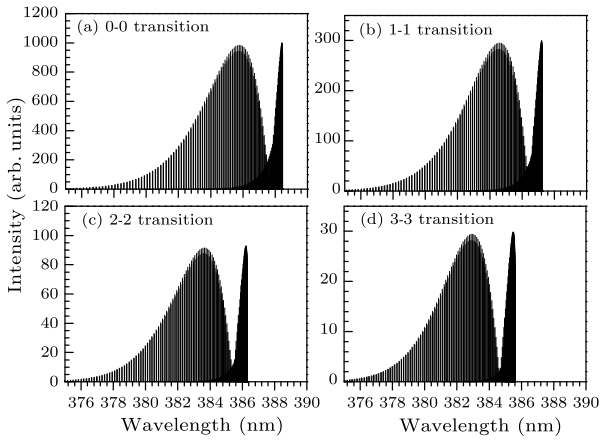

Fig. 1. Spectral line intensity distribution of the $B^2\sum^+ \to X^2\sum^+$ band at $T_e = T_v = T_r = 3000$ K.

Figure 2 indicates the dependence of intensity distribution of the $B^2\sum^+ \to X^2\sum^+$ band of the CN radical on RT, VT, and OAF. Figure 2(a) shows the total spectra and the four components for vibrational transition with $T_v = T_r = 3000$ K, where the band head from 387.6 nm to 388.8 nm is attributed to 0-0 vibrational transition and the spectral intensities whose wavelength is shorter than 387.6 nm are related to all vibrational transitions. Figure 2(b) shows a group of simulated spectra with an RT of 3000 K and various VTs of 2000, 3000, 4000, 5000 and 6000 K. It is easy to see that the spectral intensities outside the band head are obviously proportional to VT. In Fig. 2(c), a group of simulated spectra is displayed, where VT is fixed at 3000 K and RTs are set at 2000, 3000, 4000, 5000 and 6000 K. By comparing Fig. 2(c) with Fig. 2(b), the sensitivities of the second peak intensity ($\lambda \approx 387.2$ nm) and the third peak ($\lambda \approx 386.2$ nm) to RT are lower than those of the two peak intensities to VT. Finally, a variety of simulated spectra for $\Delta = 0.1$, 0.2, 0.4, 0.6 nm and $T_v = T_r = 3000$ K are given in Fig. 2(d). It can be seen that the relationship between intensity distribution and OAF is sensitive. From the above analysis, we know that the RT and VT can be estimated by analyzing the intensity distribution of the $B^2\sum^+ \to X^2\sum^+$ band of the CN radical.

In the experiment, the intensity distribution of the $B^2\sum^+ \to X^2\sum^+$ band of the CN radical is utilized to determine the RT and VT of a plasma induced by the interaction of a focused laser pulse from a free oscillated Nd:YAG laser with a coal target. The experimental setup is shown in Fig. 3. The distance between the lens and the coal target surface heated is nearly equal to the focal length of the lens, 150 mm. It is well known that the interaction mentioned above can abate some rigid granules from the coal target and a hot particle jet, which contains some free electrons formed. The seed electrons absorb the laser pulse energy through the inverse bremsstrahlung process, some of the air molecules are ionized by their collision with these accelerated electrons, the electron and ion densities all increase rapidly and a plasma forms in the front of the target surface heated.[26]

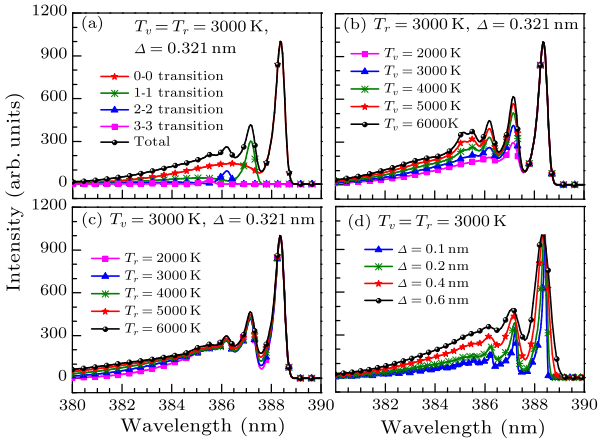

Fig. 2. Dependence of intensity distribution on RT, VT and OAF of the $B^2\sum^+ \to X^2\sum^+$ band of the CN radical: (a) the total spectrum and spectral components for four vibrational transitions; (b), (c) and (d) the groups of the total spectra for a different VT, RT and OAF, respectively.

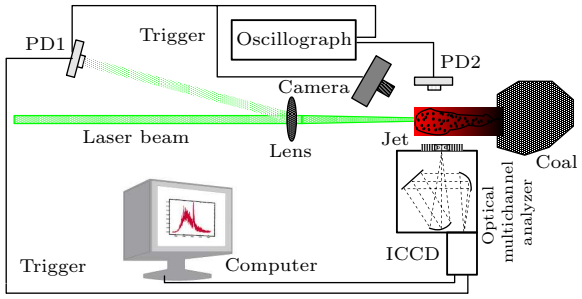

Fig. 3. Experimental setup for the interaction of a focused free-oscillated laser pulse with a coal target in air.

A four-frame CCD camera is utilized to record the images of the plasma in succession. The height and width of the images are 18 mm and 24 mm, respectively and the exposure time of each image is 20 μs. In the experiments, the appearance of the laser pulse acts as the trigger signal for the four-frame CCD camera and the delay time ΔT of every frame can be set up.

An optical multi-channel analyzer is utilized to record the spectrum of the $B^2\sum^+ \to X^2\sum^+$ band of the CN radical. Before the experiment, the mercury lamp and tungsten lamp are utilized to measure

the OAF and response of optical multi-channel analyzer, respectively. The experimental results reveal that OAF can be well fitted to a Gaussian profile and half-width is about 0.321 nm. The appearance of the laser pulse acts as the trigger signal for an optical multi-channel analyzer.

Figure 4 shows the images of plasma induced by the interaction of laser pulse with the coal target for different delay times and the energy of laser pulse is about 250 mJ. From the images, it is easy to see that the intensity of the plasma gradually expands during the laser pulse and then decreases, which is also used to prove the reliability of temperature measurement results. In addition, the experimental results also reveal that the plasma bulk is proportional to the energy of the laser pulse.

In Fig. 5, the RT and VT of the CN radical are obtained by fitting the profile of the experimental spectra of the $B^2\sum^+ \rightarrow X^2\sum^+$ band to that of the simulated spectra. The profiles in the solid lines are the experimental spectra of the $B^2\sum^+ \rightarrow X^2\sum^+$ band at different delay times and the energy of the laser pulse is about 250 mJ and the exposure time of the optical multi-channel analyzer is 4 μs. To determine RT and VT, several numerical calculations are performed for the fitting of the simulated spectra with the experimental results. The profiles in the dotted line in Fig. 5 represent the corresponding simulated spectra which are as functions of RT and VT and approach to the experimental spectra under a special RT and VT. Therefore, the corresponding values are recognized as the RT and VT of plasma.

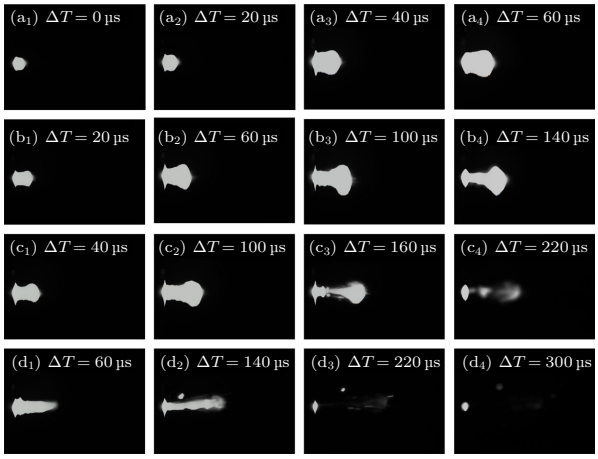

Fig. 4. Images of plasma for different delay times as energy of the laser pulse is about 250 mJ.

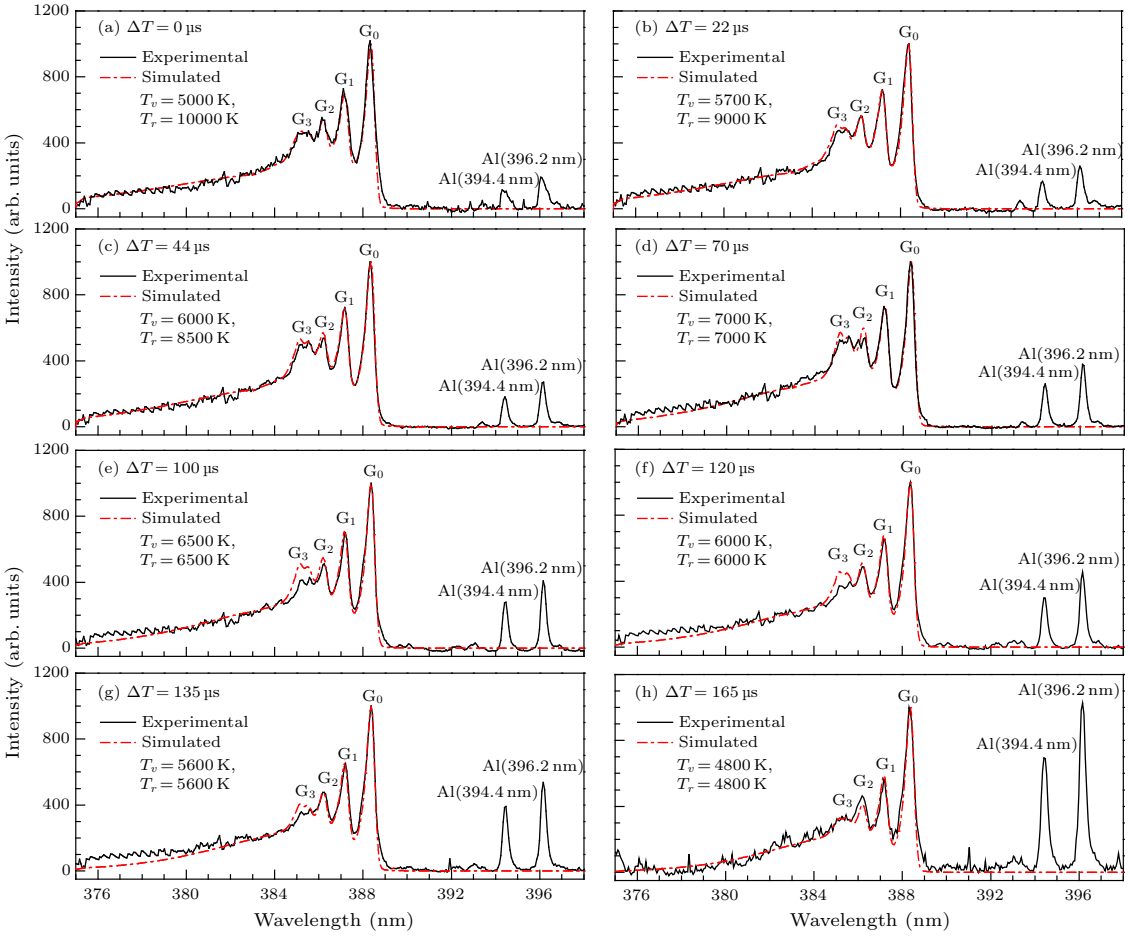

Fig. 5. Experimental spectra and corresponding simulated spectra of the $B^2\sum^+ \rightarrow X^2\sum^+$ band of the CN radials in the plasma induced by the interaction of the free-oscillated laser pulses with the coal target, where RT and VT are chosen so that the two kinds of spectra match as much as possible ($E = 250$ mJ, $\Delta = 0.321$ nm, ΔT is the delay time).

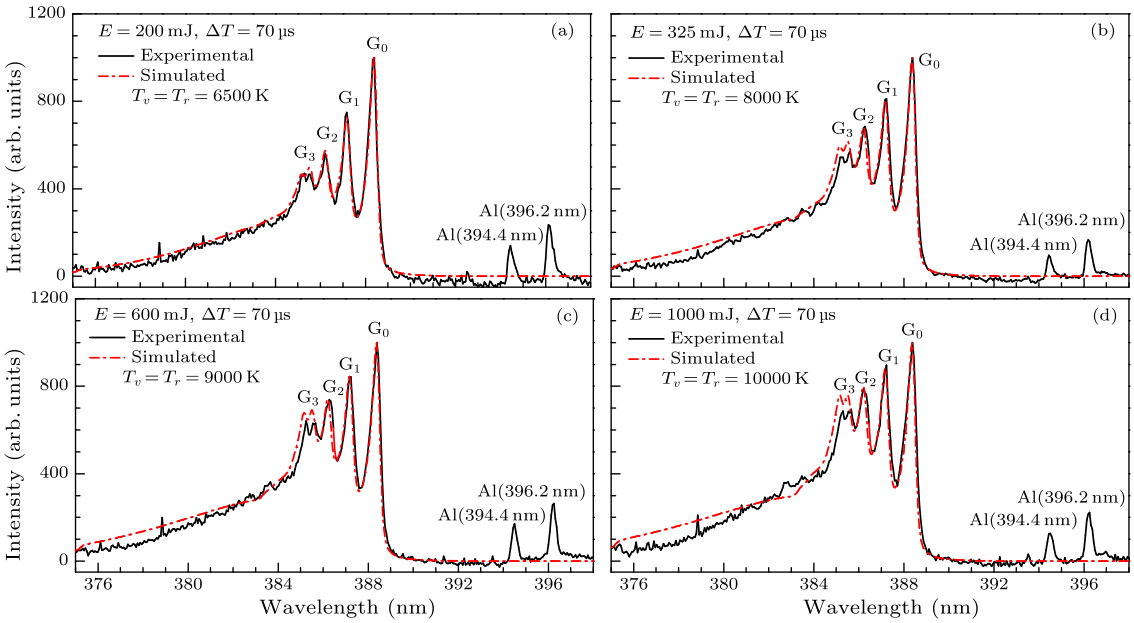

Fig. 6. Experimental spectra and the corresponding simulatin spectra of the $B^2\sum^+ \rightarrow X^2\sum^+$ band of the CN radials in the plasma induced by the interaction of the free-oscillated laser pulses with the coal target, where RT and VT are chosen so that the two kinds of spectra match as much as possible ($\Delta T = 70\,\mu$s, $\Delta = 0.321$ nm, E is the energy of the laser pulse).

The experimental data reveal that the RT of the plasma is as high as 10000 K at the beginning and the VT is about 5000 K. Then the RT decreases and VT increases, the experimental data also reveal that RT and VT of plasma reach equilibrium saturation at the delay time of 70 μs and the value is about 7000 K. After that time, the RT and VT decrease in a similar rate and the RT and VT of the plasma fall to 4800 K at the delay time of 165 μs. Compared Fig. 4 with Fig. 5, the experimental results indicate that the changing process of the temperature is similar to the evolutionary process of the plasma. In addition, the two temperatures of the plasma are proportional to the level of laser energy as shown in Fig. 6.

In summary, the characteristics of the intensity distribution of the $B^2\sum^+ \rightarrow X^2\sum^+$ band of the CN radical and its dependences on RT, VT and OAF are analyzed by numerical simulation. The two temperatures of plasma, which are induced by the interaction of a free-oscillated laser pulse with a coal target, are measured. The theoretical and numerical results reveal that the dependences of intensity distribution on the RT, VT and OAF are sensitive. In the experimental measurement, the RT and VT of the plasma are successfully determined by the fitting of the simulated spectra to the experimental spectra of the $B^2\sum^+ \rightarrow X^2\sum^+$ band.

References

[1] Chauveau S, Perrin M Y, Riviere P and Soufiani A 2002 *J. Quant. Spectrosc. Radiat. Transfer* **72** 503
[2] Laux C O and Gessman R J 2001 *J. Quant. Spectrosc. Radiat. Transfer* **68** 473
[3] Harvel E B and Carl D S 1992 *AIAA* paper 3030
[4] Kenichi A, Tsuyoshi K and Hisashi K 2005 *J. Thermophys. Heat Transfer* **19** 428
[5] Rond C, Boubert P, Félio J M and Chikhaoui A 2006 *AIAA* paper 3240
[6] Brandis A M and Morgan R G 2008 *AIAA* paper 4136
[7] Bose D, Wright M J, Bogdanoff D W, Raiche G A and Allen G A 2006 *J. Thermophys. Heat Transfer* **20** 220
[8] Lee E S, Chul P and Chang K S 2007 *J. Thermophys. Heat Transfer* **21** 50
[9] Rond C, Boubert P, Félio J M and Chikhaoui A 2007 *J. Thermophys. Heat Transfer* **21** 638
[10] Rond C and Boubert P 2009 *J. Thermophys. Heat Transfer* **23** 72
[11] Anokhin E M, Ivanova T Y, Koudriavtsev N and Starikovskii A Y 2007 *AIAA* paper 814
[12] Hyun S Y, Chul P and Chang K S 2009 *J. Thermophys. Heat Transfer* **23** 226
[13] Hyun S Y, Chul P and Chang K S 2008 *AIAA* paper 1276
[14] Djameel R, Michel D and Raymond B 1999 *J. Thermophys. Heat Transfer* **13** 219
[15] Kazuhisa F, Toshiyuki S, Masahito M and Kenji F 2008 *AIAA* paper 1254
[16] Michael W and Georg H 2008 *AIAA* paper 1212
[17] Lino D S and Dudeck M 2004 *AIAA* paper 2157
[18] Sharma S P and Whiting E E 1996 *J. Thermophys. Heat Transfer* **10** 385
[19] Lago V, Lebehot A, Dudeck M, Pellerin S, Renault T and Echegut P 2001 *J. Thermophys. Heat Transfer* **15** 168
[20] Herzberg G H 1983 *Molecular Spectra and Molecular Structure: Spectra of Diatomic Molecules* (Beijing: Science Press) chap 4 p 110
[21] Ram R S, Davis S P, Wallace L, Engleman R, Appadoo D R T and Bernath P F 2006 *J. Mol. Spectrosc.* **237** 225
[22] Dieke G H and Crosswhite H M 1962 *J. Quant. Spectrosc. Radiat. Transfer* **2** 97
[23] Jorge L and David R C 1996 *J. Chem. Phys.* **104** 2146
[24] Jorge L and David R C 1996 *J. Chem. Phys.* **104** 3907
[25] Charles D I 2000 *J. Phys. D: Appl. Phys.* **33** 1697
[26] Yang Q S, Liu C, Peng Z M and Zhu N Y 2009 *Chin. Phys. Lett.* **26** 065204